

## Rheological device

Nicola Sgambelluri, Enzo P. Scilingo, Rocco Rizzo, and Antonio Bicchi

University of Pisa

Interdepartmental Research Centre “E. Piaggio”

Italy

{n.sgambelluri, e.scilingo, r.rizzo, bicchi} @ing.unipi.it

<http://www.piaggio.cci.unipi.it>

**Summary.** In this work we investigate the possibility of mimicking haptic perception by using rheological materials. An analysis of the rheological behaviour of some “smart fluids”, such as Electro-rheological Fluids (ERFs) and Magneto-rheological Fluids (MRFs), is provided to design new haptic interfaces capable of reproducing shape and compliance of some virtual objects. Some theoretical design considerations are discussed and supported by magnetic simulations implemented by means of a numerical code. Several prototypes were designed and realized through a progressive enhancement of performance up to a final 3D immersive device. Furthermore, to assess performance a set of psychophysical tests was carried out and experimental results in terms of softness and shape recognition are reported.

### 7.1 Introduction

The present work proposes a viable solution for improving haptic perception in virtual environments, providing a haptic display capable of mimicking the softness and shape of some viscoelastic materials, such as biological tissues. Our goal was to investigate the possibility of using the smart fluids for mimicking the compliance, damping and creep (in other terms, the rheology) of some materials in order to realize haptic displays.

The main innovation concerns the direct interaction with the fluid without rigid linkages and mechanical constraints. This approach is mainly motivated by the fact that the viscoelasticity of some materials and, i.e. biological tissues, is comparable to the that of most commercial rheological fluids.

One of the most pressing limitations of commercial haptic devices is the operator’s loss of tactile sensibility during manipulation tasks due to the transmission mechanism used during the interaction. The operator may manipulate the virtual objects and by only using long tools, observing actions and movements on a monitor displaying the virtual environment (VE) . He can neither touch nor see the virtual object directly. Diminished tactile sensibility causes a loss of discrimination capability, particularly with regard to the softness and viscoelasticity of the object.

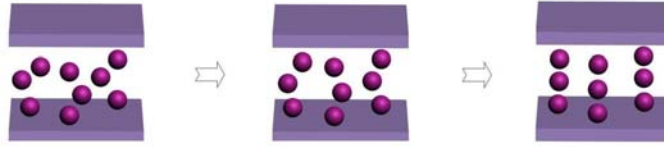


**Fig. 7.1.** Internal configuration of the ERF/MRF in the absence of the electric/magnetic field (left), in intermediate configuration (middle) and with a high electric/magnetic field applied (right).

In such a way the use of these rheological fluids as direct haptic displays could be a viable solution in important applications such as surgical training in Minimally Invasive Surgery (MIS) and Open Surgery (OS). Indeed, in MIS the MRF could be used as haptic interface to be integrated in the surgical tool in order to provide the surgeon with the lost tactile perception. In OS the MRF could be used, instead, to virtually create the internal organs of the abdominal cavity allowing the trainee surgeon to learn their compliance from palpating them.

In MIS, a small-sized MRF-based display could be a helpful means for training, enhancing the operator's skills. It should be integrated into the surgical tool, suitably sensorized for implementing a feedback control (MIS) [13].

In OS, an immersive MRF-based haptic device could be used for free-hand manipulation, whereby the operator would interact with virtual replicas of complex objects or entire environments [2].

## 7.2 Rheological Materials - State of the art

Rheological fluids, also defined as controllable fluids, or rather Electro-Rheological fluids (ERFs) and Magneto-Rheological fluids (MRFs), are a specific class of “smart materials” capable of changing their rheological behaviour when an external electric or magnetic field is applied [5].

Rheological fluids are typically non-colloidal suspensions of micron-sized particles in a synthetic liquid and exhibit a rapid, reversible and controllable transition from the liquid to a near-solid state upon the application of an external field [6]. More specifically, Electrorheological fluids (ERFs) and Magnetorheological fluids (MRFs) are materials that respond to an applied electric and/or magnetic field with a change in rheological behaviour.

Commonly, this change is manifested by the development of a yield stress that monotonically increases with the applied field. Just as quickly, the fluid can be returned to its liquid state by the removal of the field, thereby being a reversible phenomenon [11].

From a phenomenological point of view in the absence of an applied field a controllable fluid exhibits a Newtonian-like behaviour and flows freely being the polarizable particles randomly distributed in the fluid 7.1. A simple equation to describe Newtonian fluid behaviour is

$$\tau = \mu \frac{dv}{dy} \quad (7.1)$$

where  $\tau$  is the shear stress exerted by the fluid,  $\mu$  is the fluid viscosity, that is a constant of proportionality, and  $\frac{dv}{dy}$  is the velocity gradient perpendicular to the direction of shear.

In the presence of an external (electric or magnetic) field the fluid does not obey this relation and it develops a precisely controllable yield stress: the polarizable particles in the gap align themselves in the same direction of the field, and created particles chains restrict the movement of the fluid. The degree of change in terms of yield stress is approximately proportional to the magnitude of the applied field. The behaviour of rheological fluids can be represented as a Bingham plastic model [3, 7, 8, 18, 19]. In this model, having variable shear stress, the plastic viscosity is defined as the slope of the measured shear stress versus shear strain rate data, and the fluid is governed by Bingham's equations:

$$\tau = \tau_0(\bullet) + \mu \frac{dv}{dy} \quad (7.2)$$

where  $\tau_0$  is yield stress induced by a magnetic ( $\bullet = H$ ) or electric field ( $\bullet = E$ ),  $\mu$  is the viscosity and  $\frac{dv}{dy}$  is the fluid share rate. ERFs are suspensions of electrically-polarizable particles, dispersed in electrically-insulating synthetic oil. Dually MRFs are synthetic water-based or oil-based suspensions of magnetically polarizable micron-sized particles. An applied external electric or magnetic field energizes respectively ERFs and MRFs producing a yield stress compatible with a rheological characteristic of some viscoelastic materials. The energization principle of the rheological fluids is shown in Fig. 7.1.

In terms of their consistency or softness, commercial available controllable fluids appear liquid in the off-state, exhibiting a comparable value of viscosity. In this condition MRFs and ERFs reveal a low viscosity.

Since the electric field is limited by the breakdown effect in ERFs, and by the magnetic saturation in MRFs, a bounded threshold of yield strength is achievable. When an electric or magnetic field is applied, the fluids turn from liquid to near solid in few milliseconds by changing significantly their apparent viscosity. We propose here, according to our goal, to realize new haptic devices by using the rheological fluids. The MRFs appeared more suitable for our applications than ERFs due to its good yield stress range and response time. Furthermore MRFs appear to have a safer excitation field than ERFs in terms of direct interaction with the specimen.

### 7.3 MRF-based Haptic Interfaces

From an operative point of view, by using the effective characteristics of the controllable fluids, we can tune the operating point of ERFs or MRFs and, consequently, the electric ( $E$ ) or magnetic ( $B$ ) field able to set the desired yield stress ( $\tau_0$ ).

In this section we discuss the process and the rules for designing and building new haptic devices capable of properly energizing the MRFs.

A heuristic approach to designing and implementing the MRF-based devices is reported and then analyzed.

We envisioned two different configurations of MRF-based displays, the Pinch Grasp (PG) device and the Haptic Black Box (HBB) configuration.

In the former, the MRF specimen is positioned within the air-gap of an electromagnet allowing pinch grasp manipulation. In the second scheme, which is a

immersive free-hand display, a given volume of MRF is placed into a plastic box in such a way that a hand can be introduced to freely interact with the fluid. The magnetic field applied in the fluid can be controlled varying intensity over time and space, by means of suitable electromagnetic devices.

Both schemes have been designed to focus a magnetic flux into a specified region of the MRF, maximizing the magnetic field energy in this region and minimizing the energy lost in the other regions. An accurate magnetic field profile permits to build figures with a given shape and compliance. A suitable control strategy was studied so as to make MRF capable of mimicking a wide range of rheological behaviours, within limits dictated by saturation effects in the fluid.

### 7.3.1 The Pinch Grasp (PG) display

This haptic display is capable of allowing a user to manipulate simply by using their fingers (two fingers, thumb and forefinger) a reduced MRF volume. In order to apply



**Fig. 7.2.** Pinch Grasp (PG) (left) and Haptic Black Box (HBB) (right) scenarios.

the desired magnetic field to the MRF specimen, a preliminary configuration for a non-immersive scheme (see Fig. 7.2 left) was identified. The device can be properly excited in order to mimic the compliance of virtual objects.

### 7.3.2 The Haptic Black Box (HBB) display

In this section we report another MRF-prototype of a haptic display for whole-hand immersive exploration. The ideal haptic display would allow the operator to interact with the virtual object by freely moving his or her hand without mechanical constraints, exciting sensory receptors on the operator's whole hand, rather than on just one or few fingertips or phalanges. A conceptually new typology of haptic display, the Haptic Black Box (HBB) display, is here proposed [14, 15].

A HBB can be imagined as a box in which the operator can introduce his/her bare hand, and where virtual objects materialize and move under computer control according to interactions with the operator and the VE (see 7.2 right). As mentioned

above, an application that would greatly benefit from the availability of a HBB display is clearly the training of operators to open surgery operations.

An implementation of a MRF-HBB would consist of a controlled volume in which the material properties at each point could be tuned independently by some non-intrusive means.

Clearly, a concept of a 3D-HBB is rather complicated at this illustrated stage, but, to progress towards such a challenging goal, MRFs represent an interesting and innovative technology enabling, at least, some simplified form of the 3D-HBB.

## 7.4 Finite Element Method analysis

In this part some investigations and considerations on electromagnetic systems capable of energizing magnetorheological materials were reported [4]. We performed some simulations by using a 3D numerical code MEGA [12] developed at University of Bath (UK) and based on the Finite Element Method (FEM). Such a code can take into account the **B-H** function for nonlinear materials, the leakage flux due to the presence of different magnetic paths in air, as well as the presence of different feeding coils. This code allowed to analyze the profile of the flux density **B** and other electromagnetic parameters in the interested areas.

The design simulations of MRF-based devices were implemented taking care to respect a few criteria:

- the magnetic field should be as uniform as possible within an MRF specimen in order to provide a fine rheological behaviour and to maximize the capability of discrimination of different compliances;
- the range of the magnetic field should be compatible with MRF B-H and H-shear stress curves;
- the MRF specimen should be easily accessible in order to allow the hand to tactually explore freely and to perform stress relaxation and experimental tests.

The simulation led us to define specifications relative to the number of turns and current flowing into the coils in order to produce the maximum magnetic field in the gap containing the MRF according to its saturation phenomenon.

### 7.4.1 FEM analysis and optimization of the PG display

Taking into account Hopkinson's law, the initial coil system of the preliminary PG display consists of 2400 turns of copper wire having 0.8 mm in diameter. In such a way, by using a simple linear approximation, the maximum electric current is 1.26 A necessary to produce the magnetic field desired.

The system was properly optimized by using the numerical code. The MRF is positioned in the air-gap of an electromagnet within a latex sleeve allowing the pinch grasp manipulation [2].

The optimization was obtained by implementing a 2D simulation of the system by means of the MEGA software.

The scale map in Fig. 7.3 (left) shows the magnitude of the magnetic field within the ferromagnetic core and the MRF-gap. In this simulation we fixed 5100 AT (Ampere-turns). The simulation was done in order to find the optimal structural

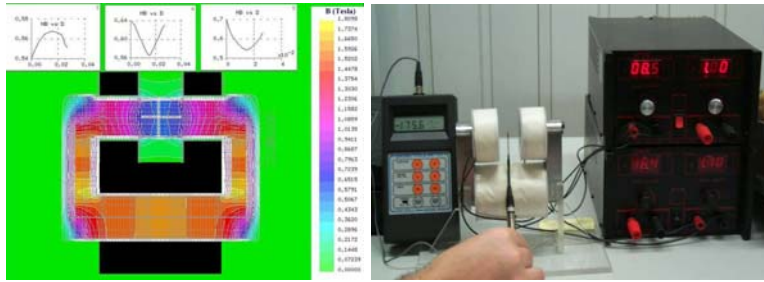


**Fig. 7.3.** Simulation (left) and experimental setup (right) of the Pinch Grasp (PG) display.

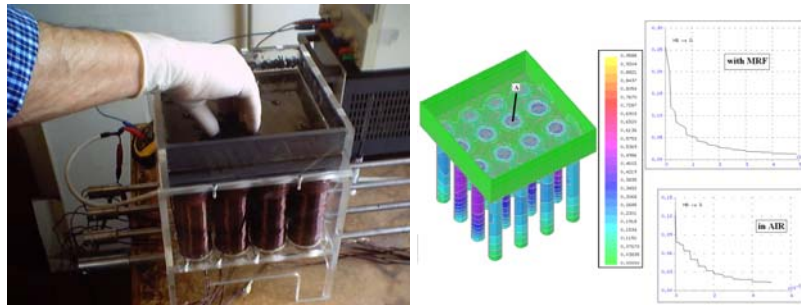


**Fig. 7.4.** Preliminary HBB-I prototype (left) and FEM simulation (right).

parameters/geometries and to reach a compromise between the distribution of the magnetic field and the dissipated energy due to overheating. A comparison was then made between the theoretical and experimental values of magnetic field.

#### 7.4.2 FEM analysis of the HBB-I display

The preliminary prototype of the immersive MRF-based display, named HBB-I, is shown in Fig. 7.4 (left). It consisted of 16 cylindrical ferromagnetic cores, arranged in a  $4 \times 4$  matrix form and placed below a plastic box with a square base. The magnetic field applied by tuning the current into each coil allows to materialize objects in the fluid with a given shape and compliance in a close range and having a specific resolution.

A 3D numerical analysis has been performed on this prototype and a simulation of the magnetic field distributions is reported in Fig. 7.4 (right).

The flux density  $\mathbf{B}$  was evaluated along the axis of a fixed coil (line  $A$  in Fig. 7.4 right). Then, by using a Gaussmeter some measurements were performed and the results are summarily reported in Table 7.1.

**Table 7.1. Comparison between FE analysis and experimental results.**

Distance from the base coil	Estimated $\mathbf{B}$ [T]	Measured $\mathbf{B}$ [T]	Error [%]
0 mm	0.15 T	0.146 T	3%
2 mm	0.13 T	0.12 T	8%
10 mm	0.06 T	0.057 T	5%

It can be seen that the maximum percentage error is about 8%, showing a good agreement between the simulated field and measured one. The results show that the magnitude of flux density  $\mathbf{B}$ , just outside the coil base, immediately decreases and at 1 cm far from the box base the field is reduced about 65% with MRF ( $\Rightarrow \mu_r = 5$ ).

#### 7.4.3 From the HBB-I to HBB-II

As a result of the FEM simulations, it is possible to report some considerations on the main problems encountered on the HBB-I device [1].

A critical point regards the paths of the magnetic flux that close themselves in air increase the magnetic reluctance and, consequently, decrease the magnetic field inside the MRF [15]. However, some possible solutions for increasing the performance of the whole system are:

- reduction of the reluctance of the magnetic paths by the introduction of ferromagnetic yokes and cores, properly positioned in the system to close the magnetic flux path;
- increase of the number of ferromagnetic cores below the box to achieve a suitable spatial resolution.

In order to verify real improvements of the system after implementing the solutions, specific simulations were carried out on a new possible MRF-HBB design.

We considered the saturation of the ferromagnetic materials used whose non-linearity compromises the performance of the whole system. However, the choice of special materials and the possibility of increasing the transversal section of the ferromagnetic yokes and columns could attenuate this problem.

Another design criterion regarded the dimensions of the MRF volume to be energized. As discussed above, the relative permeability of such fluids, comparable to that of air, leads to a large magnetic reluctance with a decrease of the magnetic field in the MRF. However, a compromise between an easy accessibility to the fluid, and the reduction of magnetic reluctance, allows to identify a proper height of the box. Then, it is possible to excite a parallelepiped of MRF with a two-dimensional spatial resolution. On the basis of these considerations, a new advanced device HBB-II towards 3D HBB free-hand exploration and capable of overcoming the limitations of the HBB-I was designed and built.

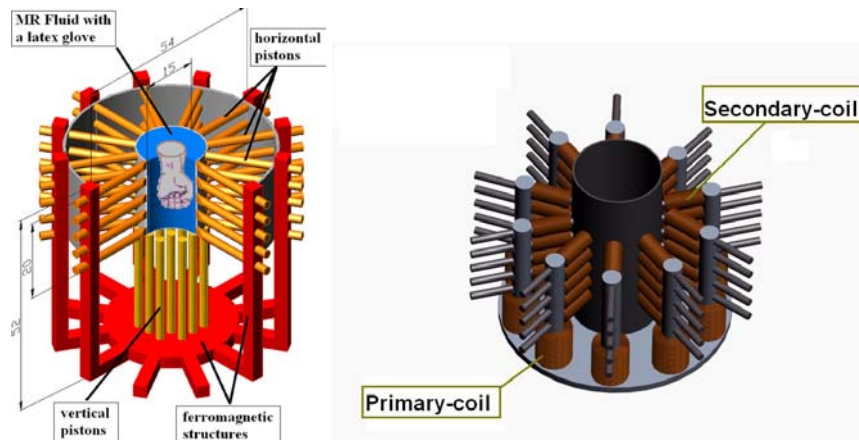


**Fig. 7.5.** Architecture of the new HBB-II device without coils (left) and with coils system (right).

### 7.5 3D HBB-II for free-hand exploration

The architecture of this new 3D display is reported in Fig. 7.5, where a schematic view of the device is shown without coils with its main dimensions (left) and the whole system (right).

It is possible to decompose the whole system in some main parts.

- **The plastic box** is used to contain the MRF and is cylindrically shaped for a better symmetry of the system. To allow free handling of the fluid, the box is internally equipped with a latex glove.
- **The ferromagnetic structure** is used to close and to address the magnetic flux. It is composed of 10 vertical columns bolted to an iron circular plate and a series of 72 "pistons", properly positioned in the system and free to move along a fixed trajectory with respect to the plastic box containing the MRF. Twenty two of such pistons are arranged in a circular matrix form below the box's base; the remaining fifty, arranged in series of  $10 \times 5$  are placed in aureole form around the lateral surface of the plastic box. They are constrained to slide in special holes present in the superior part of each column.
- **The coil system** should produce the proper magnetic field for the energization of the MRF. In the system there are two types of coils: those positioned around the inferior part of the columns and used to create the main magnetic field, the so-called *primary-coils*, and those positioned around the 72 pistons used for a fine control field resolution, the so-called *secondary-coils*. Each primary-coil is built with about 5500 AT of enamelled copper wire. The secondary-coils consist of about 2700 AT. arranged around a hollowed plastic cylindrical support. All the coils are connected to an external electronic power system to obtain the desired magnetic field in different regions of the fluid.

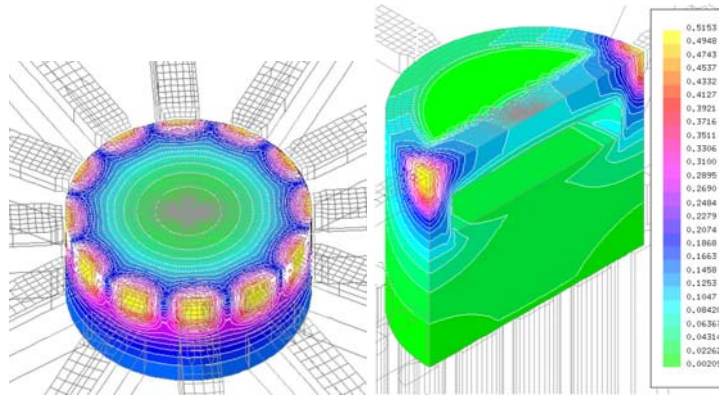


**Fig. 7.6.** Numerical simulation of HBB-II display: flux density in a generic plane when all pistons operate (left) and when 2 opposite pistons operate (right).

- **The control system** provides the current in each coil for a double purpose. From an electrical point of view it adjusts the value of current for a direct tuning of the magnetic field; from a mechanical point of view, the current in each coil allows the piston to move, inserted in the plastic cylindrical support as in a classical solenoid with a plunger inside it.

In this new configuration, in order to reduce the reluctance of the magnetic path, proper ferromagnetic yokes and cores were introduced at strategic positions. To increase the spatial resolution other smaller solenoids were arranged to create 3D virtual objects. A further improvement involved the choice of special materials AISI 1040 equipped with rubber whose nonlinearity is more attenuated. Fig. 7.6 reports the flux density in a generic plane of the fluid when all pistons are energized (left) and two opposite pistons at the same level operate (right).

### 7.5.1 Working procedure

By tuning the current in the primary-coils, it is possible to specify the rheology of the MRF. The secondary-coils that excite the mobile pistons define the active regions in the MRF and specify different compliance levels. In particular when all the mobile pistons are at rest, far from the plastic box, the reluctance of the magnetic path, closed along the line  $B - B'$  and shown in Fig. 7.7(left), is very high and the value of flux in the fluid is neglectable. On the contrary, when two or more secondary pistons are “in action” (close to the plastic box), the gap along the magnetic path  $A - A'$  is reduced implying an increase of magnetic flux in the volume of fluid corresponding to the active pistons. In such a way, it is possible to simulate many objects having different shapes and softness within the box containing the fluid.

The secondary coil system used to active the pistons, is shown in Fig. 7.7 (right). Each piston is equipped with an auxiliary mechanical device capable to move each

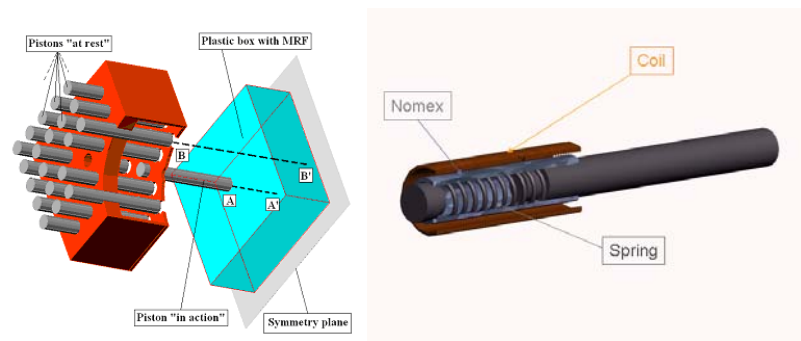


**Fig. 7.7.** Secondary-coils principle for HBB-II: pistons mechanism (left) and detail of the system (right).

piston along its axial direction when electrically energized. The auxiliary system is composed of a passive mass-spring system disposed in axial direction. The attractive magnetic force between the pistons and the MRF was simulated and its value is approximately 3.3 N for each active piston.

## 7.6 Interaction with the hand

The MRF-based devices are equipped with a latex glove allowing an unconstrained interaction between operator's hand, in the case of HBB, or fingers, in the case of PG display the the MRF. However, since the hand wearing a glove and the MRF have different magnetic characteristics, it was necessary to verify what happens during manipulation phases. For the sake of simplicity and taking into account that the formulation of the problem is similar for different devices, the analysis was studied using the PG model. The considerations and the solutions proposed can be applied to the HBB configurations.

### 7.6.1 Problem description and solutions

In order to investigate the interactions problem the analysis was performed simulating the insertion in the fluid of a little object with magnetic characteristics different from those of the fluid. From a magnetic point of view, the MRF's magnetic permeability varies in a range from 3 to 7, depending on the operating point. The inserted object perturbs the magnetic path with an increase or decrease of the magnetic flux density in the regions surrounding the object.

Fig. 7.8 shows the profiles of the magnetic flux density  $B$  in the central zone of the fluid, along two orthogonal directions x-axis (left) and y-axis (right). When the object with  $\mu_r = 1$  and  $\mu_r \gg 3-7$ . As it can be seen, for both cases, the magnetic field changes its value with respect to the absence of an object. In order to

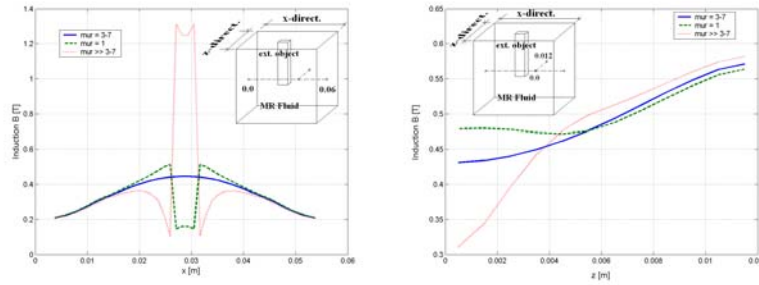


**Fig. 7.8.** Induction **B** when an object with different magnetic permeability is inserted in the fluid along x-direction (left) and along z-direction (right).

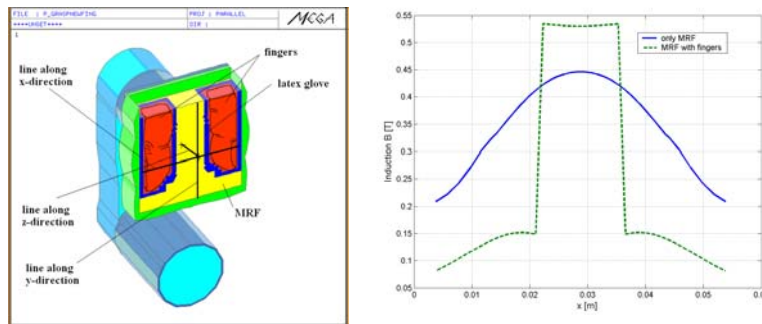


**Fig. 7.9.** Model of PG display with two fingers inserted inside the fluid (left) and its simulations along x-direction (right).

investigate a more relevant case, the system was analyzed simulating the insertion of the operator’s fingers ( $\mu_r = 1$ ) into the fluid as shown in Fig. 7.9 (left).

Fig. 7.9 (right) shows the profiles of the magnetic field along two orthogonal directions for the PG simulated models. As it can be seen, the difference between the field values in the ideal case (absence of fingers inside the fluid) and in the analyzed case (two fingers inside the fluid) is about 20–22%. Since the device should satisfy the requisite of a good field uniformity, also under different conditions, the perturbation due to the presence of objects in the fluid should be attenuated.

### 7.6.2 Interactions problem solutions

Among different implementations we proposed two solutions. The former is based on magnetic field sensors; such sensors, positioned in the fluid, are used in a feedback control system to modulate the current in the excitation coils and to compensate the

field variations due to the introduction of some objects. Although such a solution is quite general (it should be used either for  $\mu_{robj} < \mu_{rMRF}$  or  $\mu_{robj} > \mu_{rMRF}$ ) its implementation requires an auxiliary control system that could be extremely complex due to the difficulties in positioning the magnetic sensors.

The second more useful solution is based on the use of an auxiliary material, with proper magnetic characteristics, that surrounding the object inserted in the fluid, for example the operator's fingers, does not alter the magnetic equilibrium of the system.

This solution is only applicable to objects with  $\mu_{robj} < \mu_{rMRF}$  (that is the case of the operator's fingers).

In particular, it is sufficient to manufacture a glove by using a proper material. The value of the magnetic permeability  $\mu_{rx}$  of such auxiliary material has been calculated analytically. Let us consider a domain of fluid that completely surrounds the object with its cover of unknown magnetic permeability  $\mu_{rx}$ , it can be subdivided in a proper number of flux tubes. Then, calculating the magnetic reluctance of the subdomain, composed of the object with the auxiliary material, and imposing the reluctance of the subdomain like-MRF, it leads to a quadratic equation where the unknown is the magnetic permeability  $\mu_{rx}$  and the constants  $k_n$  take into account the geometry and the physical characteristics of the system.

$$k_1\mu_{rx}^2 + k_2\mu_{rx} + k_3 = 0 \quad (7.3)$$

The solutions of such equation are:  $\mu_{rx} = 10.7$  and  $\mu_{rx} = -0.23$ , with obvious choice for the first one.

### 7.6.3 The simulation results

A set of simulations of the system has been performed on the PG device considering the insertion in the fluid of the operator's fingers covered by a glove of a material with specific magnetic permeability. In Fig. 7.10, are shown the profile of magnetic induction  $B$ , in the central zone of the MRF, respectively along the  $x$  (left), and  $z$  direction (right), when two fingers are inside the fluid. As it can be seen also in Fig. 7.11 the value of  $B$  is not perturbed with respect to the ideal case without fingers in the fluid. Although from a magnetic point of view, the solution seems to show good results, this solution should be really adapted taking into account the tactile capability of the operator that should perceive any changes of shape and consistence of the MRF specimen, during the manipulation phase, without compromise the perception.

## 7.7 Psychophysical Experiments

In this section some psychophysical experiments in order to compare and to assess the performance of the MRF-based displays are considered. During the experimental session a group of subjects volunteered to perform some psychophysical tests. Each subject experimented for the first time with MRF-based devices. The experimental setup is composed of two specific phases: qualitative and quantitative analysis [9].

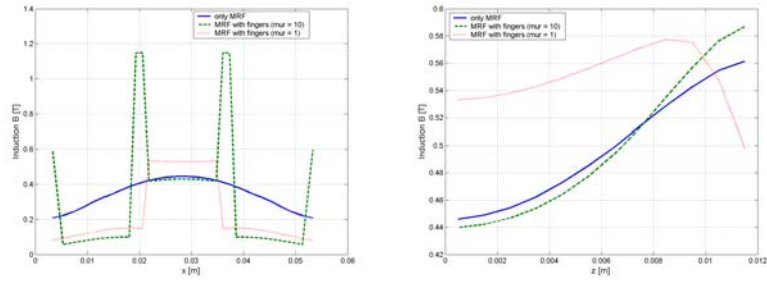


**Fig. 7.10.** Induction  $\mathbf{B}$  when two fingers are covered with a material of different magnetic permeability is inserted in the fluid (see model in Fig. 7.9) along x-direction (left) and z-direction (right).

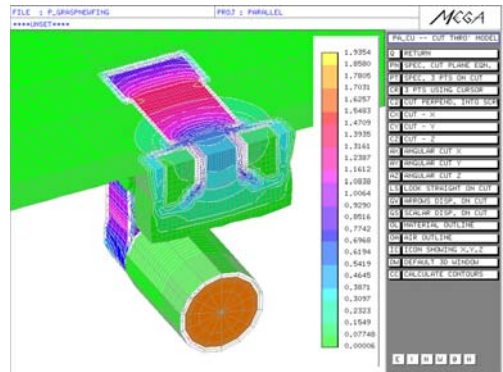


**Fig. 7.11.** Magnetic field maps inside the fluid when two fingers covered with a material of magnetic permeability=10 are inserted in the fluid.

### 7.7.1 Qualitative analysis on HBB-I

#### Position recognition

A preliminary experiment introducing the experimental session relative to shape discrimination was performed. The goal was to locate a perceived stiffer point in the HBB-I matrix. Since workspace can be represented as a  $4 \times 4$  elements of a matrix, each point is identified by a solenoid. In order to avoid providing helpful cues, a point within the box, but far from boundaries of the box was chosen by chance and the corresponding solenoid was activated. Volunteers were asked to interact with the fluid and identify the coordinates of the point perceived as stiffer (Fig. 7.12). In this preliminary version of the HBB-I the spatial resolution is quite rough. On this

account, we expected from this experiment successful results. Indeed the percentage of correct recognition was 100%. Moreover, subjects answered quickly and doubtless.

## Discussion

This experiment is a preliminary test for probing the capability of the device to allow subjects to univocally identify one point. The quite low spatial resolution of the display minimizes the probability to make a mistake in locating the point, but the entirely successful results act as a launching pad for next promising developments.



**Fig. 7.12.** Psychophysical experimental setup: top-view of the HBB-I workspace with alphanumeric coordinates of 16 quantized points (left) and real activation of one point having coordinate  $B2$  (right).

## Shape recognition and orientation detection

Another test was based on the ability of the system to produce a given shape. Two simple figures were selected and reproduced by suitably exciting a certain combination of solenoids. Volunteers were asked to manipulate the HBB-I display and freely indicate the shape perceived without receiving suggestions. The first figure reproduced was a square obtained activating four solenoids in the middle of the box (see Fig. 7.13 left). The real figure is an intermediate shape between square and circle. Subjects were asked to freely describe the figure perceived without reference frameworks. Results have to be interpreted on the basis of qualitative considerations. The figure we would reproduce was regular and symmetric and as the spatial resolution is quite low, we can accept as good all answers of the subjects referring to a geometric shape having these properties. In particular we can consider equivalent, in this context, circle, square and rectangle. We can tolerate the mistake between square and rectangle, since an uncertainty on the length side of the figure depends on the tactile artifact during the manipulation. Summarizing, 82% of the subjects recognized a figure similar to that one produced. Remaining volunteers described a regular figure but quite unlike the real figure, such as hexagon, parallelogram, rhombus, or triangle. Results are encouraging (see Fig. 7.14 left), but much work

has to be done in order to increase the spatial resolution. Afterwards, we excited three solenoids such as in see Fig. 7.13 (right). The shape of the figure so realized could be described as a triangle, L-shaped or trapezium. By assuming equivalent responses like these, we obtained results depicted in Fig. 7.14 (right). Even in this case, results can be considered satisfactory. Adding the percentages of the responses relative to L-shape, triangle and trapezium we obtain 75% of correct answers.

## Discussion

This experiment is performed in support of the possibility of reproducing an object by a given shape. The rough resolution does not help to accurately define contours, but even in this case our goal was to test the ability of the display to give an idea of the shape. Further improvements led us to have a higher resolution and a better discrimination. It has been shown in literature that during haptic exploration information regarding object properties is remarkably defined by global shape cues. Generally, shape information is easily extracted by visual means, whereas to gather this information haptically requires execution of the "contour following" exploratory procedure [10]. Our system aims at improving the softness discrimination task providing further information about the shape and the texture.

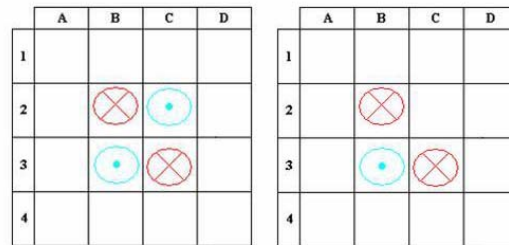


**Fig. 7.13.** Psychophysical experimental setup: set of solenoids activated in order to reproduce different shapes in HBB-I workspace: square (left) and triangle (right).

## Free shape recognition and orientation detection

This experiment is strictly correlated to the previous one. Even in this case subjects were asked to recognize the shape produced by the MRF, but now they have to choose among a predetermined set of figures (Fig. 7.15) with the addition of indicating the orientation of the figure which could be different from that represented in Fig. 7.15. Indeed, the reproduced shape could be rotated and subjects were required to indicate the orientation degree as well. Referring to Fig. 7.15 (left) shapes reproduced were I, II, IV, V, VII and VIII. The percentages of correct recognition of the shape and orientation were 76%, 96%, 85%, 80%, 81% and 93%. In Fig. 7.15

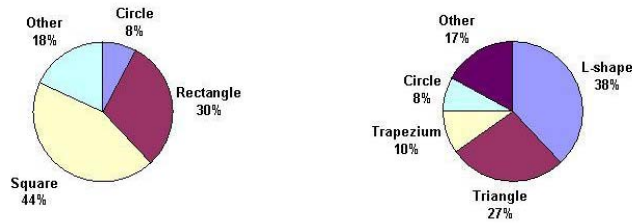


**Fig. 7.14.** Psychophysical experimental setup: pie charts showing the percentage of shapes recognized by volunteers when four contiguous solenoids (left) and three contiguous (not aligned) solenoids (right) are activated.

(right) is shown the HBB-I prototype during the emulation of the shape *V* of the set. Results are satisfactory.

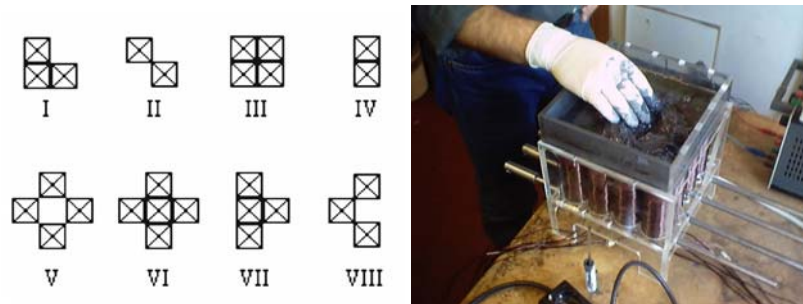


**Fig. 7.15.** Psychophysical experimental setup: set of figures from which subjects could chose the perceived shape differently oriented during the tactile manipulation of the MRF (left) and the HBB-I prototype during the experimental setup (right).

### Discussion

Some considerations have to be made. Figures II and VIII are multiply connected. Generally, a curve  $C$  in the complex plane is said to be simple if it does not cross itself. It is said to be simple closed if it is simple and its starting point and terminal point coincide. A region  $D$  in the complex plane is said to be simply connected if every simple closed curve  $C$  in  $D$  encloses only points of  $D$ , otherwise the region is

said to be multiply connected. Figures multiply connected are more easily identified than those simply connected. This is due to the ability to distinguish the geometry of different parts linked to few points. The high percentages of successful recognition are due to the fact that the shape perceived could be compared with a set of figures, since some uncertainty was easily removed by exclusion. However, this test is very significant because the changed orientation could deceive leading to errors. Therefore results were promising for next developments.

### 7.7.2 Comparison between HBB-I and PG displays

Volunteers were asked to interact with the HBB-I and/or PG displays each time and required to describe sensations perceived. Volunteers were asked to identify different level of virtual compliance/softness. Finally, few psychophysical parameters have been evaluated.

#### Compliance recognition

This experiment aimed at assessing the capability of subjects to discriminate different virtual objects by their softness. Four specimens at different compliance (Fig. 7.16) have been chosen. Since texture is a relevant cue for discriminating materials, specimens were coated with a thin layer of latex (Fig. 7.17 left). We used two different type of foam, a flock of cotton and a small ball of steel wool, all cut in the same size and shape (about 2 cm  $\times$  2 cm). The group of 50 subjects could preliminary manipulate specimens without seeing them and he was asked to rank them in terms of compliance. 100% of subjects recognized the correct stiffness scale. Next, volunteers were asked to touch the MRF displays while an assistant gradually changed the magnetic field. In the HBB-I case, only one location was excited corresponding to one solenoid (Fig. 7.17 left) in order to focus the attention only on the compliance property disregarding the shape. Subjects indicated the closest



**Fig. 7.16.** Experimental Setup: training on 4 specimens (left) and blinded test (right).

level of compliance perceived for each specimen. Through this empirical approach we

obtained a set of four virtual objects mimicked by MRFs-based displays. Once completed the calibration phase, virtual objects were submitted to volunteers in random order. To make the experiment as general as possible subjects were informed that they could be presented with virtual objects that did not belong to the specimen set, and that one repetition of the same specimen was allowed. Each trial sequence,

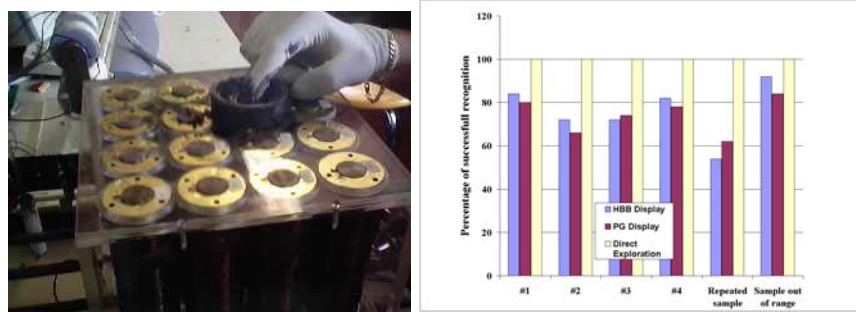


**Fig. 7.17.** HBB-I setup for softness recognition (left) and percentage of successful recognition on 6 virtual objects for HBB-I, PG displays and direct exploration (right)

therefore, implied 6 virtual objects presented to each volunteer. In Fig. 7.17 (right) the percentage of successful recognitions of the six virtual objects is reported.

## Discussion

Results are rather good for both devices. The percentage of successful recognition is on the average more than 70% for all virtual objects and for both devices. The slightly better performance of the HBB-I device can be explained by the fact that subjects could interact directly with the fluid rather than with the fluid-filled latex sleeve as in the pinch-grasp display.

## Just Noticeable Difference (JND)

Important parameters in the psychophysics of perception are absolute and differential thresholds, i.e. the minimum level of intensity of a stimulus capable of evoking a sensation, and the minimum intensity difference between two stimuli that allows the subject to distinguish between them. In the case of haptic discrimination of softness, absolute thresholds are rather difficult to measure, and not as relevant to applications as differential thresholds. We focused therefore on the assessment of the latter parameter.

The differential threshold of a perceptual stimulus, or, as it is often called, the *just noticeable difference* (JND), is a figure reflecting the fact that people are usually more sensitive to changes in weak stimuli than they are to similar changes in

stronger or more intense stimuli (for instance, one would probably notice a difference in weight between an empty paper cup and one containing a coin, yet probably a difference between a cup containing 100 coins and one containing 101 would not be noticed). The German psychophysicist Weber suggested the simple proportional law  $JND = kI$ , indicating that the differential threshold increases with increasing intensity  $I$  of the stimulus; the constant  $k$  is referred to as Weber's constant. Although more recent research indicates that Weber's law should only be regarded as a rough characterization of human sensitivity to changes in stimulation, it approximates reality well in the middle range of stimuli (the JND tends to grow more slowly in the low and high range of reference stimuli). Average values of Weber's constants are available in the psychophysical literature for most common perceptual channels, among which the two most relevant to our purposes here is for  $k = 0.013$  for diffused tactile stimuli, and  $k = 0.136$  for punctual tactile stimuli (this numbers indicate the rapid saturation of receptors involved in single-point tactile perception).

The JND is a measure of differential sensitivity, i.e. the smallest increment or decrement of stimulus for a difference to be perceived by the subject. The methodology consists in presenting a couple of stimuli and evaluate the appreciation of the difference in sensation. In order to experimentally estimate the JND versus the intensity of stimulus we used the Method of Adjustment (MOA) in which the subject adjusts the intensity until the difference in sensation is judged to be "just noticeable". For both devices, we divided the operating range of the magnetic field into 10 points. Stimulus intensity in this experiment ranged from zero to the saturation level of the MRF. Starting from each point, the magnetic field was continuously varied recording the value indicated by the subject as soon as he perceives a discrimination in sensation. Mean JND and its standard deviation for each reference stimulus was calculated for each subject, and data were averaged over the 50 subjects. Results are presented in Fig. 7.18 (left) along with the corresponding error bars.

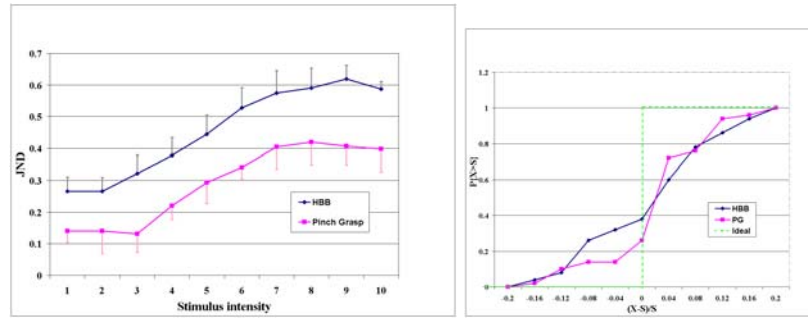


**Fig. 7.18.** Just noticeable difference versus stimulus intensity for HBB-I and PG displays (left) and Psychometric Function (right) where  $S$  is the referenced stimulus and  $X$  is the value of electric current stimulus to be compared.

## Discussion

Through linear interpolation of the middle part of the curve, it is possible to evaluate a Weber constant of 0.08 for the HBB-I display and 0.05 for the Pinch Grasp display. Average values of Weber's constants are available in the psychophysical literature for most common perceptual channels, among which the two most relevant to our purposes here are 0.013 for diffused tactile stimuli, and 0.136 for punctual tactile stimuli (this numbers indicate the rapid saturation of receptors involved in single-point tactile perception). Both Weber's fractions are hence compatible with values available in literature.

## Psychometric function

Another parameter on which we focused our attention is the psychometric function, a measure of sensorial resolution widely used in psychophysical studies. The experiment consists of asking volunteers to compare virtual compliance of the MRF in HBB-I and PG displays, in two successive trials. The working range of the magnetic field of both displays was segmented into 10 points.

In the first trial, volunteers were asked to manipulate MRF excited by the middle stimulus in the range and this is referred as reference stimulus  $S$  of compliance (by modulating the electric current of the coil). In the latter, volunteers were asked to tell whether the compliance perceived  $X$  by touching the MRF displays, if excited by a magnetic field chosen by chance within the working range, was "harder" than the reference stimulus  $S$ .

The number of positive answers divided by the total number of answers is denoted by the probability that the perceived stimulus was greater than the reference stimulus ( $P\{X > S\}$ ). As the current stimulus  $X$  was varied from lower to higher values than the reference stimulus  $S$ , the *psychometric function* was obtained as

$$F_S(X) = P\{X > S|_{(S,X)}\}. \quad (7.4)$$

In the ideal case of an infinitely fine resolution in the sensory channel, the psychometric function would be a step function ( $F_S(X) = 0, X < S, F_S(X) = 1, X > S$ ). Results are reported in Fig. 7.18 (right).

## Discussion

In order to keep the subject from knowing which intensity of the stimulus to expect from trial to trial (e.g. either a slightly stronger stimulus, in ascending series, or a slightly weaker one, in descending series we adopted the Method of Constant Stimuli (MOCS). In this case the order of presentation of the stimulus is randomized, so the subject cannot guess in advance the intensity of the stimulus. The discrepancy between the ideal step function and the experiments can be quantified by the sum of the squares of deviations from the ideal, stepwise curve, namely by the figure:

$$D = \sum_{i=1}^5 P_i^2 + \sum_{i=6}^{11} (1 - P_i)^2. \quad (7.5)$$

In the ideal case this figure is equal to zero. In real case a device is as effective about sensorial resolution as this figure approaches zero. The HBB-I display shows a parameter  $D$  equal to 0.55, while the PG display attains 0.26.

From this plot it is also possible to determine the Point of Subjective Equality (PSE) and the JND at the standard stimulus. The PSE is the length of the variable stimulus that you would judge equal to the Standard 50%. PSE is equal to 5.1 for both PG and HBB-I displays. The difference between PSE and the objective point of equality is called the Constant Error. In our case the algebraic difference between the PSE and the Standard Stimulus is equal to 0.1 for both HBB-I and PG displays. The Constant Error reflects how large the illusion is from standard conditions of the experiment. It is also possible use the plot in Fig. 7.18 (right) to determine Difference Thresholds. These thresholds indicate the amount by which a particular stimulus must be changed in order for it to be just noticeably different. The JND is obtained subtracting the stimulus judged longer 75% of the times by that judged longer 25% of the times and dividing the result by two. JND is equal to 0.2 and 0.4 for PG and HBB-I, respectively. This result (calculated at the reference stimulus) is in harmony with the general behaviour of JND calculated in Fig. 7.18 (left) for a larger stimuli range. In order to compare the psychometric functions of the two displays, we preferred to give the  $D$  factor, because it provides information about the entire selected range of stimuli. Instead, the JND and the PSE extrapolated from the psychometric function give just information about a particular stimulus chosen as reference.

### Improvements of the HBB-II

The experimental session on HBB-I entailed tests on the capability of recognizing different shape and compliance of virtual objects variously oriented. Analogous qualitative and quantitative experiments have been performed on HBB-II and a comparative investigation aiming at emphasizing the improvements has been done. Fig. 7.19 (left) illustrates the prototype HBB-II during the experimental setup. Both devices permit to identify a region perceived as stiffer within a referenced workspace with a negligible margin of error. The major difference pro HBB-II is related to a larger 3D workspace.

It is worthwhile pointing out that it is not possible to create an isolated stiff region inside the fluid.

This is due to the intrinsic fact that the magnetic field is solenoidal, i.e.  $\nabla \cdot B = 0$  or the equivalent integral form  $\int \int_A B \cdot dA = 0$ . In other terms given any volume element, the net magnitude of the vector components that point outward from the surface must be equal to the net magnitude of the vector components that point inward. This means that the magnetic field lines must be closed loops, or equivalently that there exist no magnetic monopoles.

The HBB-II workspace is larger than HBB-I, but the stiffer regions can be created only near the electromagnetic cores against the surfaces of the box containing the MRF [16]. Indeed, being the flow lines closed it not possible to reproduce, for example, a stiff sphere in the middle of the box, but it can be placed at the boundaries. Another test was based on the ability of the system to produce a given shape. Two simple figures were selected and reproduced by suitably exciting a certain combination of solenoids. Volunteers were asked to manipulate both HBB-I and HBB-II displays and freely describe the shape perceived without receiving suggestions. Even

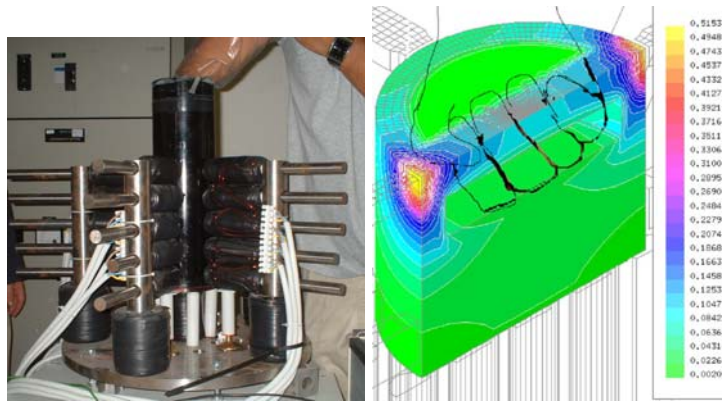


**Fig. 7.19.** Prototype HBB-II during the experimental setup (left) and numerical simulation of a cylinder shape with the HBB-II when 2 opposite pistons operate (right).

in this case both devices provided satisfactory results, but while figures created by HBB-I were constrained to be confined at the bottom of the box, HBB-II was able to produce a 3D virtual object which could be totally and freely grasped by the hand. In particular volunteers easily recognized a cylinder positioned at different orientations or radial patterns as shown in Fig. 7.19 (right).

Clearly, definition and accuracy of the virtual figures are strictly correlated to the spatial resolution of the device which is higher in HBB-II. The final experiment aimed at assessing the capability of subjects to discriminate different virtual objects by their softness. HBB-I in this case is more limited due to smaller range of magnetic field which can be produced. The novel architecture of HBB-II allowed to attain the saturation level of MRF thus exploiting all the dynamics and discriminating an increased number of virtual object by softness [17].

### 7.7.3 Discussion

These psychophysical tests, showed that the new device, HBB-II is more effective than its predecessor. The improvements included the increasing of the number of solenoids and the reduction of their sizes that resulted in a higher spatial resolution. The most important novelty with the HBB-II concerns the possibility of creating 3D virtual objects with an augmented tactile perception.

## 7.8 Conclusions

In this paper we explored the possibility of implementing haptic interfaces by using MRFs. Unlike kinesthetic displays present in literature this type of haptic interface would allow a direct contact with a compliant object. In this case both kinesthetic

and cutaneous channels of the fingerpads are stimulated during the manipulation and tactile perception is augmented. Two different architectures of haptic display based on MRFs are envisioned: a non-immersive Pinch Grasp display and a free-hand Haptic Black Box device.

The design phase was supported by numerical FEM analysis to optimize the performance of both devices. Moreover, a new 3D-HBB based on MRFs allowing subject to manipulate 3D virtual objects was designed and realized.

Performance of all the systems here proposed were assessed through psychophysical tests showing satisfactory results. Future developments could progress towards the possibility of creating dynamic figures changing with time and space.

## Acknowledgments

This work is part of the TOUCH-HapSys project financially supported by the 5th Framework IST Programme of the European Union, action line IST-2002-6.1.1, contract number IST-2001-38040. For the content of this paper the authors are solely responsible for, it does not necessarily represent the opinion of the European Community.

## References

1. Bicchi A, Raugi M, Rizzo R, and Sgambelluri N (2005) IEEE T Magn 41(5):1876–1879.
2. Bicchi A, Scilingo E P, Sgambelluri N, De Rossi D (2002). Haptic Interfaces based on magnetorheological fluid, In: Proceedings 2th International Conference Eurohaptics 2002, 6–11.
3. Bossis G and Lemaire E (1991) J RHEOL 35(7):1345–1354.
4. Brooks N, Baldwin T (2002). Methodology for universal synthesis of magnetic designs based on field specifications. In: Proc. of the Thirty-Fourth Southeastern Symposium on System Theory, 113–117.
5. Carlson J D, Catanzarite D N and St Clair K A (1996). Commercial Magneto-Rheological Fluid Device. In: Proceedings 5th Int. Conf. on ER Fluids, MR Suspensions and Associated Technology, 20–28.
6. Choi S B, Choi Y T, Park D W and Lee H G (1998). Smart Structures and Integrated Systems. In: Proc. of SPIE - The International Society for Optical Engineering, Smart Structures and Materials, 3329:439–450.
7. Fedorov V A (1992) Magnetohydrodynamics 28(1):96.
8. Kabakov A M and Pabat A I (1990) Sov Electr Eng 26(2):99-104.
9. Klatzky R A, Lederman S, and Reed C (1987) J Exp Psychol Gen 116(4):356-369.
10. Lederman S J, and Klatzky R L (1987) , Cognitive Psychol 19:342-368.
11. <http://www.lord.com>
12. MEGA, User Manual, Bath University, UK, Nov. 2000.
13. Scilingo E P, Bicchi A, De Rossi D, Scotto A (2000). A magnetorheological fluid as a haptic display to replicate perceived compliance of biological tissues. In: 1st Annual Int. IEEE-EMBS Special Topic Conference on Microtechnologies in Medicine & Biology, 12–14.

14. Scilingo E P, Sgambelluri N, De Rossi D, Bicchi A (2003). Haptic Displays Based on Magnetorheological Fluids: Design, Realization and Psychophysical Validation. In: 11th Symposium on Haptic Interfaces for Virtual Environment and Teleoperator Systems, 10–15.
15. Scilingo E P, Sgambelluri N, De Rossi D, Bicchi A (2003). Towards a Haptic Black Box: Magnetorheological fluid based display for softness and shape discrimination. In: IEEE Int. Conf. on Robotics and Automation, 2412–2417.
16. Sgambelluri N, Rizzo R, Scilingo E P, Raugi M, and Bicchi A (2006). Free Hand Haptic Interfaces Based on Magnetorheological Fluids. In: Proc. 14th Symp. on Haptic Interfaces for Virtual Environment and Teleoperator Systems 367–371.
17. Sgambelluri N, Scilingo E P, Bicchi A, Rizzo R, and Raugi M (2006). Advanced Modeling and preliminary psychophysical experiments for a free-hand haptic device. In: IEEE/RSJ Int. Conf. on Robots and Intelligent Systems, 1558–1563.
18. Spencer B F, Dyke S J, Sain M K and Carlson J D (1997) J Eng Mech Div-ASCE 123:230–238.
19. Spronston J L, Yanyo L C, Carlson J D, El Wahed A K (2002). Controllable Fluids in 2002 - Status of ER and MR technology. In: 8th International Conference on New Actuators & 2nd International Exhibition on Smart Actuators and Drive Systems, 333–338.